DOI: 10.1007/s10288-006-2029-2

Numerical simulation of air-water two-phase flow over stepped spillways

CHENG Xiangju[1], CHEN Yongcan[1] & LUO Lin[2]

1. Department of Hydraulic Engineering, Tsinghua University, Beijing 100084, China;
2. State Key Laboratory of Hydraulics and Mountain River Engineering, Sichuan University, Chengdu 610065, China

Correspondence should be addressed to Cheng Xiangju (email: chengxj@tsinghua.edu.cn)

Received April 19, 2005; accepted August 16, 2006

Abstract Stepped spillways for significant energy dissipation along the chute have gained interest and popularity among researchers and dam engineers. Due to the complexity of air-water two-phase flow over stepped spillways, the finite volume computational fluid dynamics module of the FLUENT software was used to simulate the main characteristics of the flow. Adopting the RNG k-ε turbulence model, the mixture flow model for air-water two-phase flow was used to simulate the flow field over stepped spillway with the PISO arithmetic technique. The numerical result successfully reproduced the complex flow over a stepped spillway of an experiment case, including the interaction between entrained air bubbles and cavity recirculation in the skimming flow regime, velocity distribution and the pressure profiles on the step surface as well. The result is helpful for understanding the detailed information about energy dissipation over stepped spillways.

Keywords: stepped spillway, mixture model, RNG k-ε model, air-water two-phase flow.

Stepped spillways have been used for about 3500 years[1] because of the ease of construction and design simplicity. By the end of the 20th century, it was understood that stepped spillways contributed significantly to the dissipation of the hydraulic energy, for example in the design of the Monksville dam and Upper Stillwater dam[2]. Energy dissipation occurs by momentum transfer or the transmission of turbulent shear stress between the skimming stream and the horizontal-axis re-circulating vortices over the stepped spillways. Many studies[3,4] found that favorable design of stepped spillways can decrease the size of stilling basin significantly, or rather leave out stilling basin, leading to cheaper construction costs. Therefore designers need to know the accurate velocity, pressure and air concentration distribution of flow over stepped spillways in advance. Many relevant studies performed with hydraulic models and field investigations were effective[5,6]; however they are expensive and time consuming. Moreover, it is almost impossible to keep simultaneously the three analogue parameters, the Froude, Weber and

Reynolds numbers, as the same value. Today, with the use of high-performance computers and more efficient computational fluid dynamics (CFD) codes, the behavior of flow structures can be investigated numerically in reasonable time and with reasonable expense.

The complicated air-water two-phase flow will be formed under the strong action of the steps' disturbing nappe over spillways and the majority of the air will be trapped into water. Currently, the mixture model is very popular to simulate the characteristics of air-water two-phase flow. Two-phase flows are taken as continuous mediums and coupled by the means of their interactions in the mixture model because the mixture model allows for the modeling of multiple, separate, yet interacting phases. Choudhury[7] introduced the theory of Renormalization Group (RNG) into the study of turbulent flow and developed RNG k-ε model. Compared with the standard k-ε model, the RNG k-ε model is better suited for simulating separated and re-circulating flows.

Introducing the mixture model for air-water two-phase flow, the RNG k-ε model was used to compute the flow field over a stepped spillway. The numerical results are compared with the experimental data.

1 Description of physical model

A physical model of a typical WES spillway provided by Chen[8] is shown in Fig. 1. The design head is $H_d = 9.7$ cm. The model was made of plexiglas and fabricated to conform to the distinctive shape of a WES crest, which was described by the equation $y = 3.632x^{1.85}$. Three arc segments with different radii were up to the vertical upstream face and the radii equaled to 4.85, 1.94 and 0.388 cm respectively. Below the tangency point T, the spillway profile had a slope of $1V:0.75H$, completed by an ogee with a radius of 28 cm down to the horizontal channel at the toe. On the whole spillway, there were 13 steps, which were numbered 1 to 13, from the top to the bottom. The h represented the vertical distance above the horizontal surface of the step, and the l represented the horizontal distance from the vertical surface of the step. The first five steps were transition steps and had a variable height-to-length ratio, so that the envelope of the step tips followed the spillway profile. The heights of the first three steps were 2, 2.4 and 3 cm above the tangency point. The heights of the other two transition steps were 4 and 5 cm below the tangency point. Below the step No. 5, eight uniform steps (6 cm high and 4.5 cm long) continued to the toe. The spillway crest was 82.7 cm above the toe and 30 cm wide.

The test discharge of the spillway was 30 L/s, which was measured by an orthogonal weir installed in front of the approach channel. The flow velocities were measured by using an optical fiber laser Doppler anemometer. On the horizontal and vertical surfaces of the odd numbered steps from step No. 5 to No. 13, five piezometer tubes were fixed on each vertical and horizontal step surface to measure mean pressures. Connected by a 3 mm-diameter red copper tube was inserted into the plexiglass wall of the step; the piezometers were installed in the step wall. The plexiglass depth was 5 mm. Near both ends of the step's vertical surface, the two piezometers were 5 and 9 mm from the left, and the right ends were 5 and 2 mm, respectively. In the middle, there was an equal spacing be-

tween two adjacent piezometers. The equipments were shown in the refs. [8, 9].

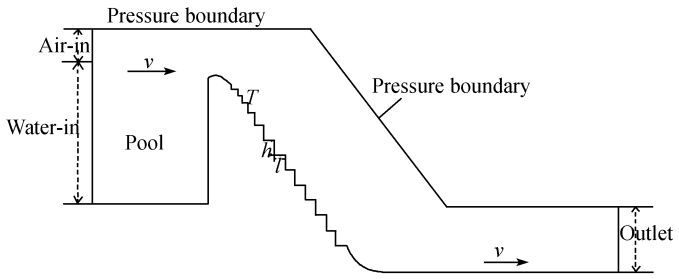

Fig. 1. The calculation domain and boundary conditions.

2 Mixture model of air-water two-phase flow

The mixture model differs from the volume of fluid (VOF) model in three respects: (i) The mixture model allows the phases to be interpenetrating. The volume fractions α_k and α_q for a control volume can therefore be equal to any value between 0 and 1, depending on the space occupied by phase k and phase q. (ii) The mixture model allows the phases to move at different velocities, using the concept of slip velocities. (iii) There is interaction of the inter-phase mass, momentum and energy transfer in the mixture model. However, the VOF method does not compute the dynamics in the void or air regions. This paper hypothesizes that air bubbles distribute in water uniformly, and water body cannot be gasified. The mixture model equations are derived in the ref. [10].

2.1 Continuity equation for the mixture flow

$$\frac{\partial \rho_{\mathrm{m}}}{\partial t} + \nabla \cdot (\rho_{\mathrm{m}} \boldsymbol{u}_{\mathrm{m}}) = 0, \tag{1}$$

where the mixture density and the mixture velocity are defined as

$$\rho_{\mathrm{m}} = \sum_{k=1}^{n} \alpha_k \rho_k \,, \tag{2}$$

$$\boldsymbol{u}_{\mathrm{m}} = \frac{1}{\rho_{\mathrm{m}}} \sum_{k=1}^{n} \alpha_k \rho_k \boldsymbol{u}_k \,, \tag{3}$$

where α_k and ρ_k are the volume fraction and density of phase k, respectively. The mixture velocity $\boldsymbol{u}_{\mathrm{m}}$ represents the velocity of the mass centre of the mixture flow. Note that ρ_{m} may vary even though the component densities keep constant.

2.2 Momentum equation for the mixture flow

In terms of the mixture variables, the momentum equation takes the form

$$\frac{\partial}{\partial t} \rho_{\mathrm{m}} \boldsymbol{u}_{\mathrm{m}} + \nabla \cdot (\rho_{\mathrm{m}} \boldsymbol{u}_{\mathrm{m}} \boldsymbol{u}_{\mathrm{m}}) = -\nabla p_{\mathrm{m}} + \nabla \cdot (\tau_{\mathrm{m}} + \tau_{\mathrm{Dm}}) + \nabla \cdot (\mu_{\mathrm{eff}} \nabla \boldsymbol{u}_{\mathrm{m}}) + \rho_{\mathrm{m}} g. \tag{4}$$

The two stress tensors are defined as

$$\tau_{\mathrm{m}} = \sum_{k=1}^{n} \alpha_k \mu_{\mathrm{eff}} \nabla \boldsymbol{u}_k , \tag{5}$$

$$\tau_{\mathrm{Dm}} = -\sum_{k=1}^{n} \alpha_k \rho_k \boldsymbol{u}_{\mathrm{M}k} \boldsymbol{u}_{\mathrm{M}k} , \tag{6}$$

where $\boldsymbol{u}_{\mathrm{M}k}$ is the diffusion velocity for the mixture flow. The two stress tensors represent respectively the average viscous stress and diffusion stress due to the phases slip. In eq. (4) the pressure of the mixture flow is defined by the relation

$$\nabla p_{\mathrm{m}} = \sum_{k=1}^{n} \alpha_k \nabla p_k . \tag{7}$$

In practice, the phase pressures are often taken to be equal, *i.e.* $p_k = p_{\mathrm{m}}$.

2.3 Continuity equation for phase k

From the continuity equation for secondary phase *k*, the volume fraction equation for secondary phase *k* can be obtained

$$\frac{\partial}{\partial t}(\alpha_k \rho_k) + \nabla \cdot (\alpha_k \rho_k \boldsymbol{u}_{\mathrm{m}}) = -\nabla \cdot (\alpha_k \rho_k \boldsymbol{u}_{\mathrm{M}k}). \tag{8}$$

2.4 The relative velocity

Before solving the continuity eq. (8) for phase *k* and the momentum eq. (4) for the mixture, the diffusion velocity $\boldsymbol{u}_{\mathrm{M}k}$ has to be determined. The diffusion velocity of a phase is usually caused by the density differences, resulting in forces on the bubbles different from those on the fluid. The additional force is balanced by the drag force.

$$\boldsymbol{u}_{\mathrm{M}k} = \boldsymbol{u}_{qk} - \sum_{k=1}^{n} \frac{\alpha_k \rho_k}{\rho_{\mathrm{m}}} \boldsymbol{u}_{qk} , \tag{9}$$

where $\boldsymbol{u}_{qk}$ is the slip velocity between air and water, defined as the velocity of air relative to the velocity of water. Following Manninen *et al*.[11], $\boldsymbol{u}_{qk}$ is defined as

$$\boldsymbol{u}_{qk} = \frac{(\rho_{\mathrm{m}} - \rho_k) d_k^2}{18 \mu_{\mathrm{eff,m}} f_{\mathrm{drag}}} \left[g - (\boldsymbol{u}_{\mathrm{m}} \cdot \nabla) \boldsymbol{u}_{\mathrm{m}} - \frac{\partial \boldsymbol{u}_{\mathrm{m}}}{\partial t} \right], \tag{10}$$

where $\mu_{\mathrm{eff,m}}$ is the effective viscosity of mixture and d_k is the diameter of the particles (or bubbles) of secondary phase *k*. The bubble diameter used in the simulation is 5 mm. Reasonable agreement with the experimental data of Cummings[12] is obtained by using this bubble diameter value. The drag function f_{drag} is taken from Clift *et al*.[13]:

$$f_{\mathrm{drag}} = \begin{cases} 1 + 0.15 Re^{0.687} & Re \leqslant 1000, \\ 0.0182 Re & Re > 1000. \end{cases} \tag{11}$$

3 RNG k-ε model for the mixture flow

The RNG-based k-ε turbulence model is derived from the instantaneous Navier-Stokes

equations, using a mathematical technique called "renormalization group" (RNG) method.

The k-ε equations describing the mixture flow are as follows:

$$\frac{\partial}{\partial t}(\rho_{\mathrm{m}}k)+\nabla\cdot(\rho_{\mathrm{m}}\boldsymbol{u}_{\mathrm{m}}k)=\nabla\cdot\left(\frac{\mu_{\mathrm{eff,m}}}{\sigma_k}\nabla k\right)+G_{k,\mathrm{m}}-\rho_{\mathrm{m}}\varepsilon, \tag{12}$$

$$\frac{\partial}{\partial t}(\rho_{\mathrm{m}}\varepsilon)+\nabla\cdot(\rho_{\mathrm{m}}\boldsymbol{u}_{\mathrm{m}}\varepsilon)=\nabla\cdot\left(\frac{\mu_{\mathrm{eff,m}}}{\sigma_\varepsilon}\nabla\varepsilon\right)+C_{1\varepsilon}\frac{\varepsilon}{k}G_{k,\mathrm{m}}-C_{2\varepsilon}^{*}\rho_{\mathrm{m}}\frac{\varepsilon^2}{k}, \tag{13}$$

where k is the turbulence kinetic energy, and ε is referred to dissipation rate of k.

$$\mu_{\mathrm{eff,m}}=\mu_{\mathrm{m}}\left[1+\sqrt{\frac{C_\mu}{\mu_{\mathrm{m}}}}\frac{k}{\sqrt{\varepsilon}}\right]^2, \tag{14}$$

where μ_{m} is the molecular viscosity of mixture.

$G_{k,\mathrm{m}}$ represents the generation of turbulence kinetic energy due to the mean velocity gradients, calculated as

$$G_{k,\mathrm{m}}=\mu_{t,\mathrm{m}}\left[\nabla\boldsymbol{u}_{\mathrm{m}}+(\nabla\boldsymbol{u}_{\mathrm{m}})^T\right]\nabla\boldsymbol{u}_{\mathrm{m}}. \tag{15}$$

$C_{2\varepsilon}^{*}$ is given by

$$C_{2\varepsilon}^{*}\equiv C_{2\varepsilon}+\frac{C_\mu\rho\eta^3(1-\eta/\eta_0)}{1+\beta\eta^3}. \tag{16}$$

$\eta\equiv Sk/\varepsilon$, $S=\sqrt{2\bar{S}_{ij}\bar{S}_{ij}}$ is the modulus of the mean rate of strain tensor expressed as

$$\bar{S}_{ij}=\frac{1}{2}\left(\nabla\boldsymbol{u}_{\mathrm{m}}+(\nabla\boldsymbol{u}_{\mathrm{m}})^T\right). \tag{17}$$

The values of the constants in above equations are $C_\mu=0.0845$, $C_{1\varepsilon}=1.42$, $C_{2\varepsilon}=1.68$, $\sigma_k=\sigma_\varepsilon=0.75$, $\eta_0=4.38$, $\beta=0.012$.

4 Solution of the numerical models

4.1 Numerical methods

The computational fluid dynamics module of the FLUENT version 6.2 was utilized to model the flow over the stepped spillway. FLUENT is a general finite volume code that can be used to model a wide range of fluid-flow problems. The control-volume-based technique was used to solve the equations. The calculation domain was divided into discrete control volumes by the unstructured grid which has a high flexibility to fit the complex geometry and boundary of stepped spillway. The convective fluxes in the mean volume fraction, momentum and turbulence closure equations were discretized by employing a conservative, second-order accurate upwind scheme. The pressure-velocity coupling algorithm is the pressure-implicit with splitting of operators (PISO), which is based on the higher degree of the approximate relation between the corrections for pressure and velocity[14] and may also be useful for transient calculations on highly skewed

meshes.

4.2 Boundary conditions

The boundaries are shown in Fig. 1. The inlet section consisted of the inlet of water on the lower part and the inlet of air on the higher part upstream of the dam. The water inflow velocity can be calculated according to the discharge and the water depth at the water inlet. The air boundary was set as pressure-inlet conditions on which atmospheric pressure was assumed. Because the boundary between water and air at the downstream outlet could not be distinguished, it was defined as a pressure boundary, or free-flow condition. All of the walls were set as the stationary, non-slip wall. The viscosity layer near to the wall dealt with the standard wall function. The initial flow field over the stepped spillway was full of air. Through the time-dependent simulation, the water flowed over the spillway and produced air-water two-phase flow.

5 Simulation results and analysis

The experimental data by Chen[8] were used for the validation of the air-water two-phase flow simulations over the stepped spillway. The comparison includes the air-water mixture velocity distribution, air entrainment and the static pressure profiles along the stepped spillway.

5.1 The air-water mixture velocity distribution

Fig. 2 shows the measured and calculated velocity vector distributions on step No. 6. The correspondence is good enough for the velocity magnitude and the location and size of the eddy in the steps to support the numerical simulation. Seen from the Fig. 2, eddies rotated clockwise and their centers were about 1.2 cm above the horizontal surface of the step No. 6. Fig. 2 also shows that the velocity increases from the center of eddies to the flow surface.

Fig. 3 shows the velocity distributions at different sections of step No. 7 and 9 for experiments and simulations. The agreement in each section is excellent. It can also be seen from Fig. 3 that the velocity profiles for each step are similar (others are not shown herein). The section where coordinate x is equal to 1.1 cm, at the viscosity layer near to the horizontal surface, shows that the velocity is almost equal to zero. Along the vertical surface, the air-water mixture velocity decreases continuously until reaching a minimum value at a point. Near the water surface, the air-water mixture velocity reaches its maximum level.

5.2 The air entrainment

Fig. 4 shows the air entrainment simulated by the mixture model and experimented in a laboratory. The simulated result (Fig. 4(a)) reflects vividly the air entrainment pattern compared with the picture of the experiment (Fig. 4(b)). The flow behavior on a stepped spillway was divided by many researchers[15,16] into two types: nappe flow regime and skimming flow regime. Nappe flow occurs normally for low discharges and shallow flows while skimming flow occurs for high discharges and deep flows. As shown in Fig.

4, the flow behavior belongs to skimming flow. Water flowed down the stepped face as a coherent stream, skimmed over the steps and was cushioned by the re-circulated fluid trapped between the steps. Along the upstream steps, free-surface aeration took place when the outer edge of the boundary layer reached the free-surface. Energy dissipation occurred due to momentum transfer between the skimming stream and the vortices.

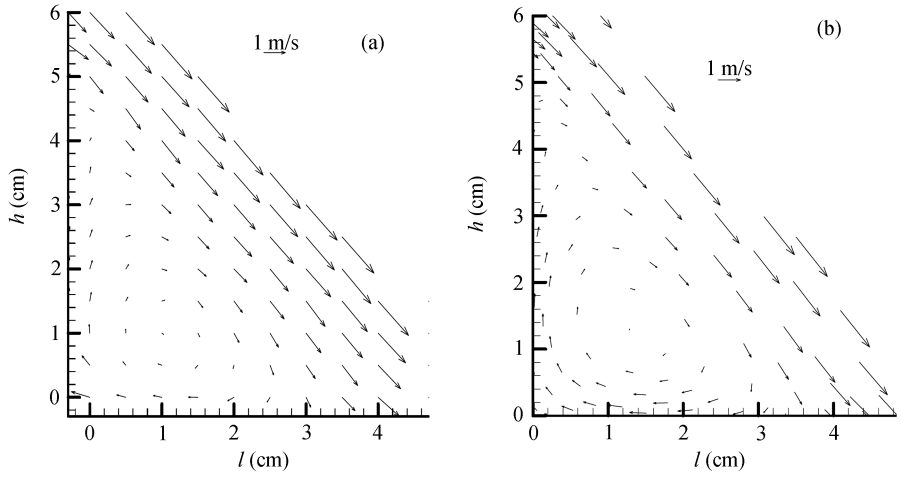

Fig. 2. Measured and calculated velocity on step No. 6. (a) Measured; (b) simulated.

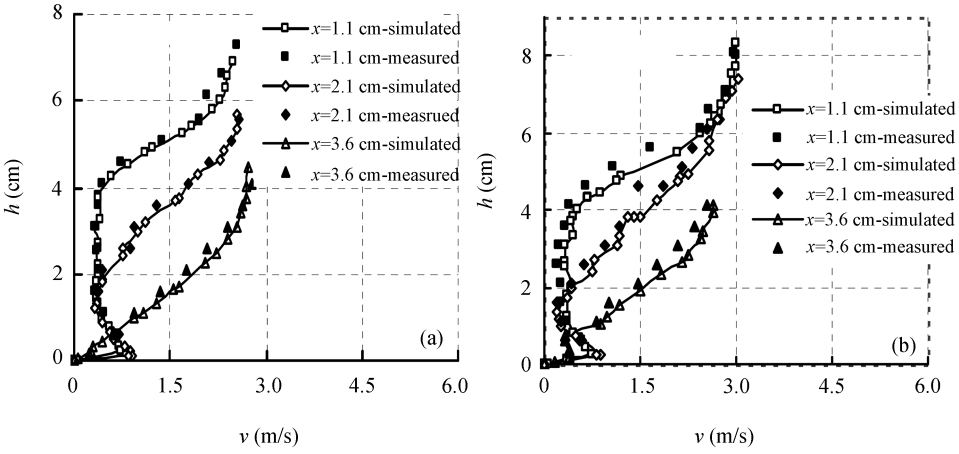

Fig. 3. Velocity distribution on step No. 7 (a) and No. 9 (b).

The available data on the inception of air entrainment were analyzed[17] so the inception point location can be expressed as functions of Froude number containing the unit discharge and step height and chute angle. Seen from the Fig. 4, the location of the inception of air entrainment is clearly shown on step No. 5, and the inception point location simulated by numerical methods is in agreement with the location measured by experiment. At the inception point, the degree of turbulence was large enough to entrain air into the black water flow. A main advantage of the significant aeration along stepped spillways is the reduction of the cavitation risk potential. For high velocities, the hydrodynamic pressures on the step surfaces or at the step edges may fall below the vapor pres-

sure, resulting in cavitation which might cause severe damage to the spillway concrete. Based on the fundamental work of Peterka[18], a bottom air concentration of about 5%–8% was considered sufficient to avoid cavitation damage because the compressibility of the air-water mixture can absorb the impact of collapsing vaporized bubbles. Knowing the location of the inception point is thus important to determine the un-aerated spillway zone, which is potentially prone to cavitation damage. Although steps form large offsets on the boundary, the placement of an aerator in the black water region of a stepped spillway to artificially entrain air might be of interest.

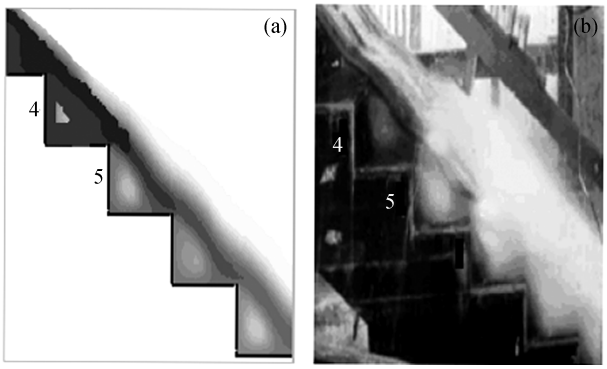

Fig. 4. Air entrainment over the stepped spillway. (a) Calculated; (b) measured.

5.3 The pressure profiles

Fig. 5 shows the pressure profiles on the horizontal and vertical surfaces on steps No. 5, 7, 9 and 11, respectively. It can be seen that the simulated values of pressure fit the experimental results well. On the horizontal surface, the pressure decreases slightly, then increases to the maximum and decreases again at the step tip. The maximum pressure is caused by the impact of the flow. Along the vertical surface, the pressure is minimum near the top and maximum near the bottom. There are negative pressures near the top of the vertical surface in the simulated results and the maximum negative pressure equals to 0.5 kPa. Fig. 6 shows the negative pressure profile simulated by numerical methods on the step tips (others are not shown herein). It can be seen that there are negative pressures on all of the tips of the steps. The negative pressure has importance for the assessment of cavitations potential. In fact, the step tips will be possibly destroyed because of the negative pressure. In laboratory, it is very difficult to measure the negative pressure without specific equipment. However, the numerical method in this paper can be easily used to simulate the negative pressure distribution over each step tip. It can be concluded that thenumerical method in this paper can be a supplemental tool for the assessment of cavitations potential.

6 Conclusions

The following findings of the present numerical study apply:

(i) The mixture model for air-water two-phase flow and RNG k-ε turbulence model are

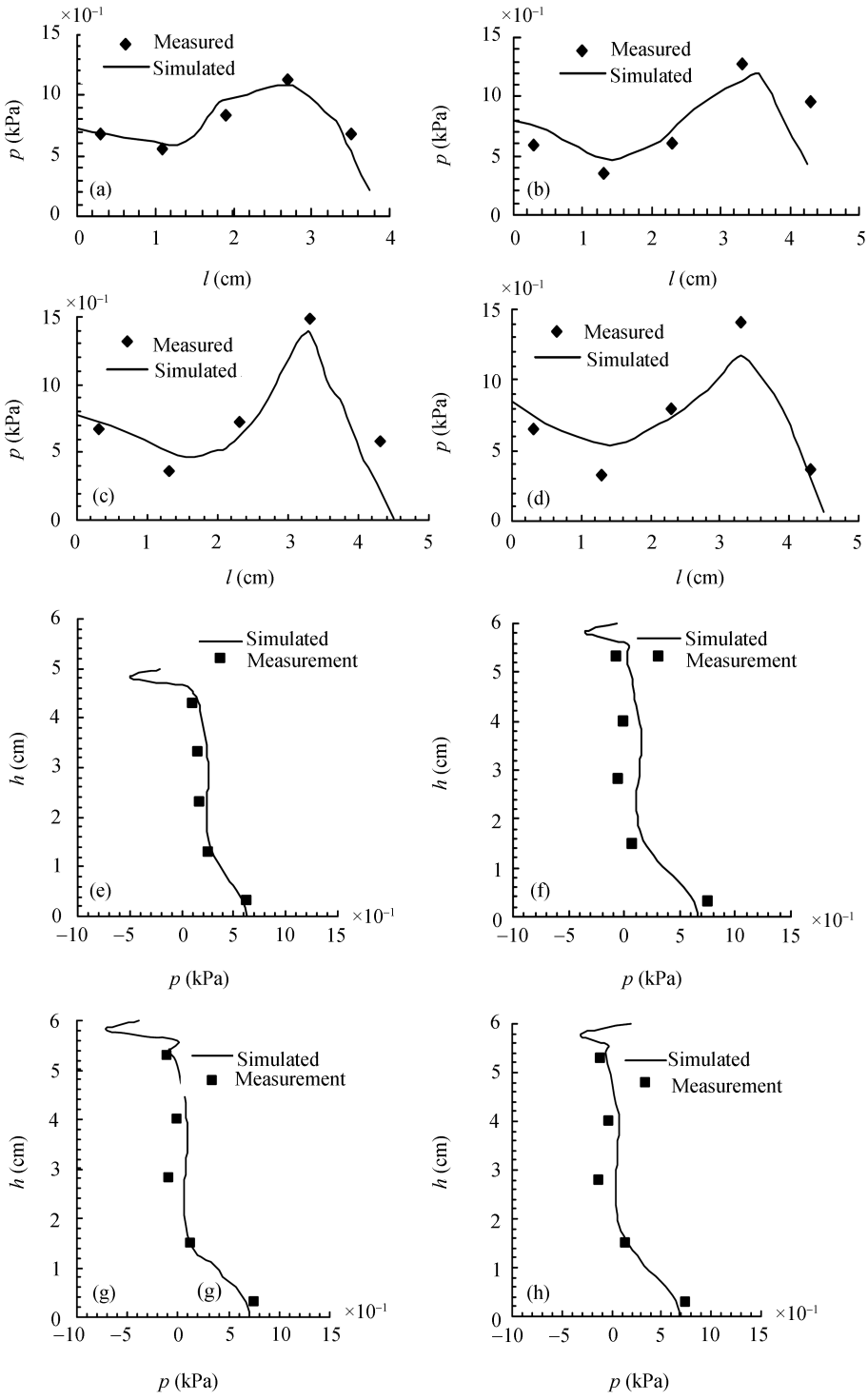

Fig. 5. Pressure profile on step's surface. (a), (b), (c) and (d) Horizontal surface on step No. 5, 7, 9 and 11; (e), (f), (g) and (h) vertical surface on step No. 5, 7, 9 and 11.

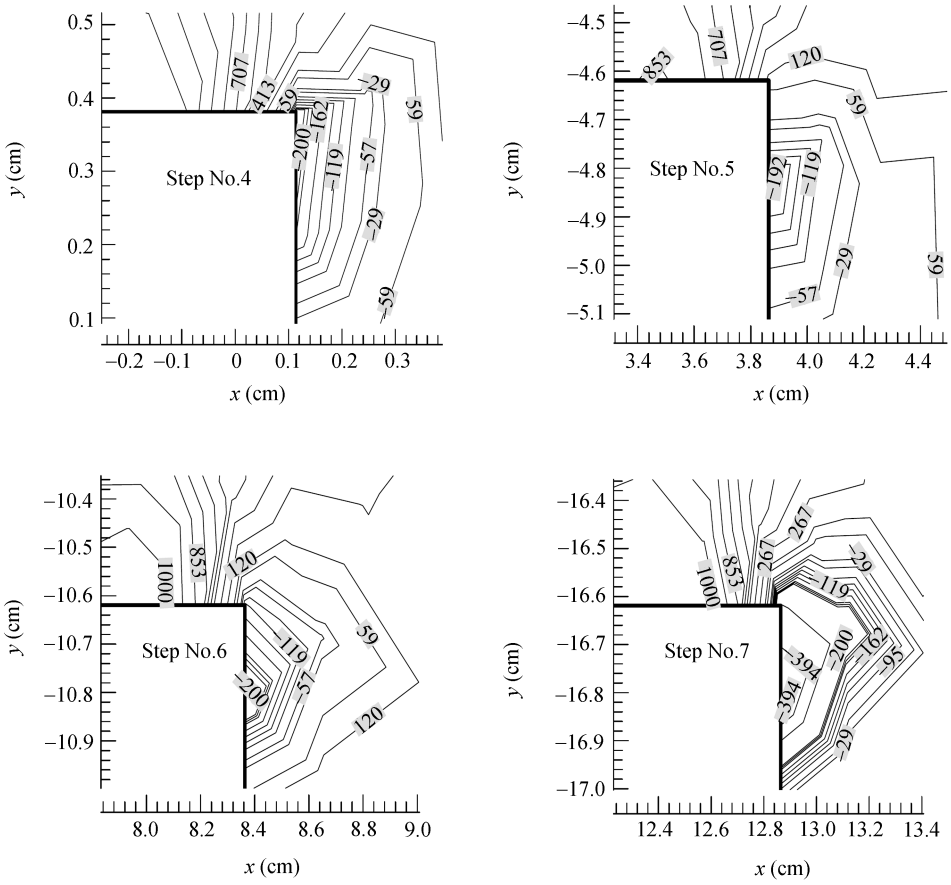

Fig. 6. Negative pressure profiles on step tips (unit: Pa).

combined to simulate successfully the flow characteristics over stepped spillways. This method, compared to other experimental methods, is more advantageous for gathering information on negative pressures. The mixture model successfully simulates the interactions between entrained air bubbles and cavity recirculation in the skimming flow regime and overcomes the limitation of the VOF model. Compared with the standard k-ε model, the RNG k-ε model is better suited for simulating these separated and re-circulated flows.

(ii) According to the simulated results, the inception point of air entrainment can be found. Downstream of this point, rapid air entrainment takes place, and "white water" and eddies appear in the corners of every step. Energy dissipation occurs by momentum transfer between the skimming stream and the vortices.

(iii) The simulated pressure profiles on the step surfaces provide the theoretical foundation for assessing the cavitations risk. In order to study the flow characteristics of stepped spillways systematically, the numerical method shows a greater advantage in practice. Moreover, the numerical method in this paper is an essential tool for the assessment of cavitations potential.

Acknowledgements This work was supported by the National Natural Science Foundation of

China (Grant No. 50609011).

References

1 Chanson H. Forum article: Hydraulics of stepped spillways. J Hydraul Eng, 2000, 126(9): 636—637
2 Hansen K D. Roller-compacted concrete developments in the USA. Water Power Dam Construction, 1986, 1: 9—12
3 Boes R M, Hager W H. Hydraulic design of stepped spillways. J Hydraul Eng, 2003, 129(9): 671—679
4 Minor H E. Spillways for high velocities. In: Zurich V E, Minor H E, Hager W H, eds. Proceedings of International Workshop on Hydraulics of Stepped Spillways, Rotterdam, the Netherlands, 2000. 3—10
5 Charles E R, Kadavy K C. Model study of a roller compacted concrete stepped spillway. J Hydraul Eng, 1996, 122(6): 292—297
6 Pagliara S, Dazzini D. Energy dissipation on stepped fall manholes. Urban Drain, 2002, 112: 315—330
7 Choudhury D. Introduction to the Renormalization Group Method and Turbulence Modeling. Fluent Inc Techn Memo TM-107, 1993. 1—30
8 Chen Q. Turbulence numerical simulation and model test of the stepped spillway overflow. Dissertation for the Doctoral Degree (in Chinese). Chengdu: Sichuan University, 2001. 21—32
9 Chen Q, Dai G Q, Liu H W. Volume of fluid model for turbulence numerical simulation of stepped spillway overflow. J Hydraul Eng, 2002, 128(7): 683—688
10 Ishii M. Thermo-fluid Dynamic Theory of Two-phase Flow. Paris: Eyrolles, 1975. 32—86
11 Manninen M, Taivassalo V, Kallio S. On the Mixture Model for Multiphase Flow. VTT Publications 288, Technical Research Centre of Finland, 1996. 1—65
12 Cummings P D, Chanson H. Air entrainment in the developing flow region of plunging jets—Part 2: Experimental. J Fluids Eng, 1997, 119(9): 603—608
13 Clift R, Grace J R, Weber M E. Bubbles, Drops, and Particles. London: Academic Press, 1978. 97—120
14 Ferzieger J L, Peric M. Computational Methods for Fluid Dynamics. Heidelberg: Springer-Verlag, 1996. 54—60
15 Chamani M R, Rajaratnam N. Onset of skimming flow on stepped spillways. J Hydraul Eng, 1999, 125(9): 969—971
16 Chanson H. Experimental investigations of air entrainment in transition and skimming flows down a stepped chute. Can J Civ Eng, 2002, 29: 145—156
17 Boes R M, Hager W H. Two-phase flow characteristics of stepped spillways. J Hydraul Eng, 2003, 129(9): 661—670
18 Peterka A J. The effect of entrained air on cavitation pitting. In: Proceedings of 5th IAHR Congress, Minneapolis, 1953. 507—518